

# Approximate depth averages of electrical conductivity from surface magnetotelluric data

E. Gómez-Treviño

*CICESE, Ciencias de la Tierra, Ensenada, Baja California, 22860 México*

Accepted 1996 August 22. Received 1996 August 9; in original form 1996 February 29

## SUMMARY

This paper presents a simple non-linear method of magnetotelluric inversion that accounts for the computation of depth averages of the electrical conductivity profile of the Earth. The method is not exact but it still preserves the non-linear character of the magnetotelluric inverse problem. The basic formula for the averages is derived from the well-known conductance equation, but instead of following the tradition of solving directly for conductivity, a solution is sought in terms of spatial averages of the conductivity distribution. Formulas for the variance and the resolution are then readily derived. In terms of Backus–Gilbert theory for linear appraisal, it is possible to inspect the classical trade-off curves between variance and resolution, but instead of resorting to linearized iterative methods the curves can be computed analytically. The stability of the averages naturally depends on their variance but this can be controlled at will. In general, the better the resolution the worse the variance. For the case of optimal resolution and worst variance, the formula for the averages reduces to the well-known Niblett–Bostick transformation. This explains why the transformation is unstable for noisy data. In this respect, the computation of averages leads naturally to a stable version of the Niblett–Bostick transformation. The performance of the method is illustrated with numerical experiments and applications to field data. These validate the formula as an approximate but useful tool for making inferences about the deep conductivity profile of the Earth, using no information or assumption other than the surface geophysical measurements.

**Key words:** electrical conductivity, electromagnetic induction, inversion, magnetotellurics.

## 1 INTRODUCTION

In the past three decades a number of methods have been developed for interpreting magnetotelluric (MT) sounding data in terms of conductivity distributions that vary only with depth. Perhaps because of the rather large number of papers on the subject, or possibly due to the apparent simplicity of the problem, it is often stated that research on one-dimensional (1-D) inverse methods is little needed, and that all efforts must be directed towards the multidimensional cases. In this respect it must be recognized that we are still to address a most fundamental question in the 1-D situation, namely the construction of a rigorous theory for making mathematically defensible inferences from the data without relying on assumptions external to the observations. The problem was highlighted by Parker (1983) in his review paper prepared for the Sixth IAGA Workshop on Electromagnetic Induction in the Earth as the most important challenge remaining in 1-D at that time. Since then, very little has been reported in the literature in the

way of attempts at its solution. The implications of the problem go far beyond those of academic interest, considering that 1-D interpretations are still widely used in shallow exploration problems and in the study of the deep structure of the Earth. The problem is perhaps most relevant in the analysis of very long-period MT soundings; there are some unique 1-D data sets that seem to indicate the existence of conductivity discontinuities in the upper mantle (e.g. Schultz *et al.* 1993; Bahr, Olsen & Shankland 1993). The defence of important results such as these calls for rigorous methods to investigate the degree of non-uniqueness inherent in the 1-D MT inverse problem. It is very likely that these data will be revisited in the light of future developments in this direction.

In mathematical terms the inference problem can be stated as the search for the common properties shared by all models fitting the observations. Most of our efforts in 1-D inversion have been directed towards the goal of fitting the observations with the response of a conductivity distribution  $\sigma(z)$ , where  $z$  represents depth. This problem is known to be ill-posed in the

sense that it allows the construction of a whole set of satisfactory conductivity models from a given set of field data. It has also been recognized that it is impossible to establish bounds on the conductivity at any given depth. For this reason, the inversion is stabilized by incorporating known or assumed properties of the conductivity structure. Examples of *a priori* constraints are the common assumption of a small number of homogeneous layers to represent the earth (e.g. Weaver & Agarwal 1993), and constraints on the depth derivative of the conductivity distribution (e.g. Constable, Parker & Constable 1987; Smith & Booker 1988). These methods usually address the problem of non-uniqueness, but only within the restricted set of models allowed by the particular constraints. For this reason they are not considered rigorous inference methods from a mathematical point of view.

General mathematical methods for solving the problem of inference have been applied to the 1-D MT problem. These include Backus–Gilbert theory for linear appraisal (Backus & Gilbert 1970), which has been applied by Parker (1970) and Oldenburg (1979) by linearizing the problem; funnel functions as described by Oldenburg (1983), also applied after linearization; and Monte Carlo methods that do not require linearization (e.g. Jones & Hutton 1979). The methods were reviewed by Parker (1983) who found that linearization is an unreliable approximation and that the Monte Carlo approach is very limited at best. The failure of these general methods called for more specific techniques designed for the particular problem at hand.

Weidelt (1985) considered the inference problem in terms of conductance bounds for an arbitrary depth  $z$ . A conductance function  $S(z)$  is defined as the integral of  $\sigma$  from the surface of the Earth down to a depth  $z$ , and the goal is to establish bounds on  $S(z)$  for all possible models that fit the data. In this case it is known that the 1-D magnetotelluric inverse problem is well posed for  $S(z)$ , as demonstrated by Dmitriev (1983). The formulation of Weidelt (1985) is rigorous, and the solution has the sufficient generality for the method to be considered as a good approximation to the general inference problem. However, as mentioned by Weidelt (1985), the more general and useful solution would be to establish bounds on the average conductivity  $\bar{\sigma}(z_1, z_2)$  in an arbitrary depth interval  $(z_1, z_2)$ .

The idea of extremizing  $\bar{\sigma}(z_1, z_2)$  was initially proposed by Parker (1983) as a possible way of approaching the general problem in a rigorous manner. Apart from the work of Oldenburg (1983), who applied the concept of funnel functions via linearization, the problem has not been examined in the literature for a decade. Recently, the problem was considered in two presentations given at the XI Workshop on Electromagnetic Induction in the Earth (Weidelt 1992; Gómez-Treviño 1992). The first was a rigorous attempt to solve the problem using non-linear programming, and the second was an analytical solution using a very simple non-linear approximation. The present work is an account of the second presentation. It is hoped that the treatment given here could increase awareness of the inference problem within a much wider circle in the electromagnetic community.

## 2 THE CONDUCTANCE EQUATION

Dmitriev (1983) presented the formal proof that the 1-D MT inverse problem is well posed for the conductance. Although

this proof is very recent, it had long been recognized that magnetotelluric measurements are more directly related to conductance than to conductivity. This was expressed mathematically by Niblett & Sayn-Wittgenstein (1960) by means of an approximate relationship between the measurements and an arbitrary conductivity distribution. They considered apparent conductivity measurements defined as

$$\sigma_a(T) = 2\pi\mu_0 T^{-1} |Z|^{-2}, \quad (1)$$

where  $\sigma_a$  represents the apparent conductivity,  $\mu_0$  the permeability of free space, and  $Z$  the electrical impedance on the surface of the Earth measured at a period  $T$ .

The relation between  $\sigma_a$  and the vertical conductivity profile was obtained by Niblett & Sayn-Wittgenstein (1960) by assuming a finite-difference approximation in Maxwell's equations. Their result can be written as

$$\sigma_a(T) = \int_0^h k_a(\sigma_a, T, z) \sigma(z) dz, \quad (2)$$

where

$$h = \left( \frac{T}{2\pi\mu_0\sigma_a} \right)^{1/2} \quad (3)$$

and

$$k_a(\sigma_a, T, z) = \begin{cases} 1/h, & z \leq h, \\ 0, & z > h. \end{cases} \quad (4)$$

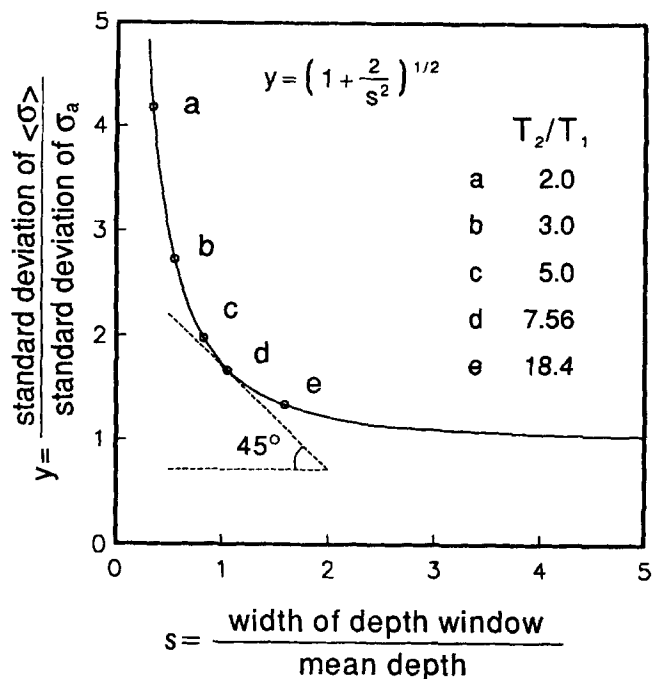


**Figure 1.** Trade-off curve of variance and resolution for a homogeneous earth. Note the steep behaviour of the curve for  $s < 1$ . This means that it is possible to lower the variance of the averages significantly without a great loss in resolution. The rule of diminishing returns begins at  $s = 1$  for which  $T_2 = 7.56T_1$ . This implies that we can take two data points almost one decade apart in period and still obtain reasonable resolution. The Niblett–Bostick transformation corresponds to  $s = 0.0$ , for which case the variance is unbounded. This explains why the transformation is unstable for noisy data.

Eq. (2) shows that  $\sigma_a$  represents the average of  $\sigma(z)$  from the surface of the Earth down to a maximum depth  $h$ . It also shows that the product  $\sigma_a h$ , which can be computed directly from the data, represents the conductance for the region  $z \leq h$ . This means that magnetotelluric measurements on the surface of the Earth are essentially conductance measurements. The conductivity profile  $\sigma(h)$  may then be recovered simply by taking the derivative of  $\sigma_a h$  with respect to  $h$ .

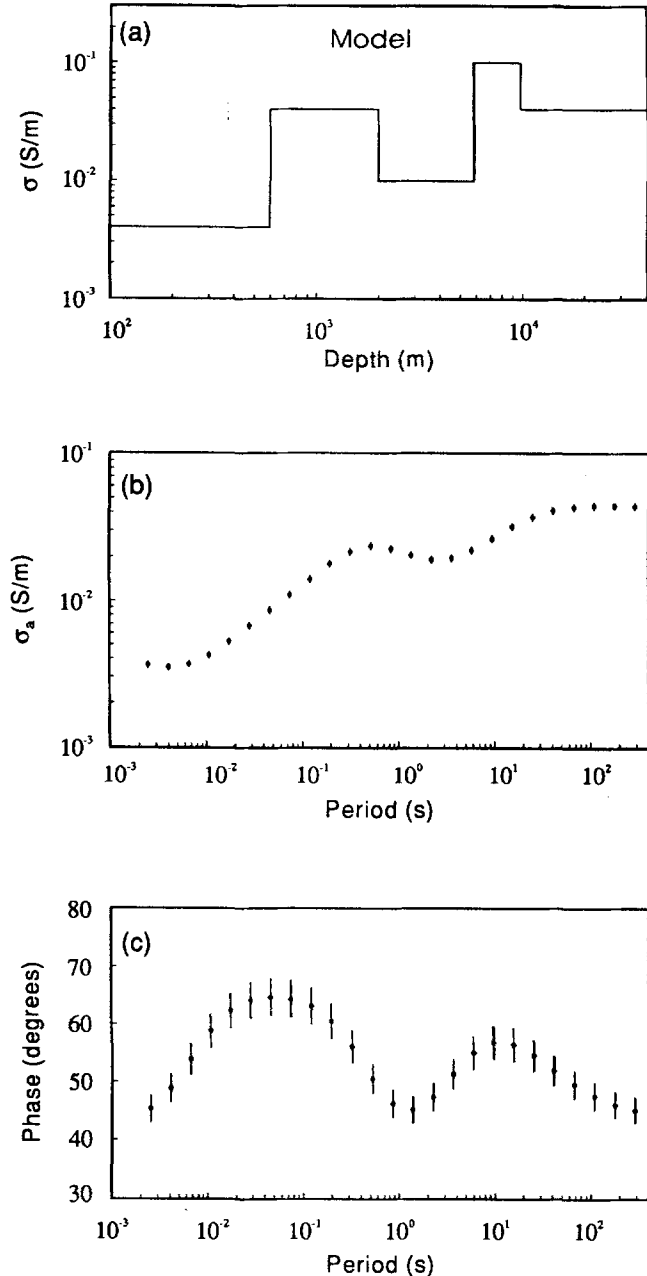


**Figure 2.** Test model and corresponding apparent conductivity and phase curves. The values of the response are noise-free but they are assigned 5 per cent error bars. In this we follow Whittall & Oldenburg (1992) who used the same model and curves to illustrate the performance of a variety of inverse methods. We use this model here to evaluate the performance of eqs (12) and (A9). The results are shown in Figs (3) and (A1).

The recovery of  $\sigma(h)$  through derivation represents an exact inversion method, in the sense that  $\sigma(h)$  is an exact solution of the non-linear integral eq. (2). This solution is known as the Niblett–Bostick transformation and is given as

$$\sigma(h) = \sigma_a(T) \frac{1+m}{1-m}, \quad (5)$$

where

$$m = \frac{\partial \log \sigma_a}{\partial \log T}. \quad (6)$$

The details of the derivation can be found in Bostick (1977) Jones (1983). An alternative proof is provided in a later section of this paper on the basis of the general formula for the average of conductivity. What is important here is simply to note that eq. (5) is not a solution of the inference problem posed in the Introduction. The inference problem needs to be formulated in its own terms in order to address the question of non-uniqueness. This is considered in the next section, after the following brief discussion about the approximate nature of eq. (2).

It is possible to get an idea of the type of approximations behind eq. (2) by comparing its kernel with the kernel of the exact conductance equation. The exact equation is derived in Gómez-Treviño (1987), and is given as:

$$\sigma_a(T) = \int_0^\infty k_e(\sigma, T, z) \sigma(z) dz, \quad (7)$$

where

$$k_e(\sigma, T, z) = \frac{1}{1-m} F(\sigma, T, z) G(\sigma, T, z), \quad (8)$$

with

$$F(\sigma, T, z) = 2 \left[ \frac{T}{2\pi\mu_0\sigma_a} \right]^{1/2} \left| \frac{E(z, T)}{E(0, T)} \right|^2 \quad (9)$$

and

$$G(\sigma, T, z) = \cos[2\phi(z, T) - \phi(0, T)]. \quad (10)$$

$E(z, T)$  is the electric field at depth  $z$ ,  $\phi(z, T)$  is the phase of  $E(z, T)$  with respect to  $B(0, T)$ , the magnetic field on the surface of the Earth, and  $m$  is as in eq. (6).

Comparing eqs (2) and (7), it turns out that the exact kernel  $k_e(\sigma, T, z)$  is approximated by the box-car function  $k_a(\sigma_a, T, z)$ . Notice that the approximation is intended to hold for all periods and for all conductivity distributions  $\sigma(z)$ , and that a rather simple function accommodates all situations. This is because the box-car function has an amplitude and depth extent adaptable for different periods and apparent conductivity values. This suffices as a first-order approximation to the exact kernel of eq. (7) because despite its complicated appearance, the exact kernel has some simple properties that follow from the well-known constraints on  $m$ ,  $\phi(0, T)$  and  $E(z, T)$ . Gómez-Treviño (1987) used this constraint and a string of arguments to reduce eq. (7) to eq. (2). The box-car function represents a compromise to accommodate the exact kernel for  $m < 0$  and  $m > 0$ . Considering that the electric field decreases with depth, an inclined straight line could be a better choice for the approximation of the exact kernels, but this would certainly complicate the derivations aimed at recovering information about the conductivity profile.

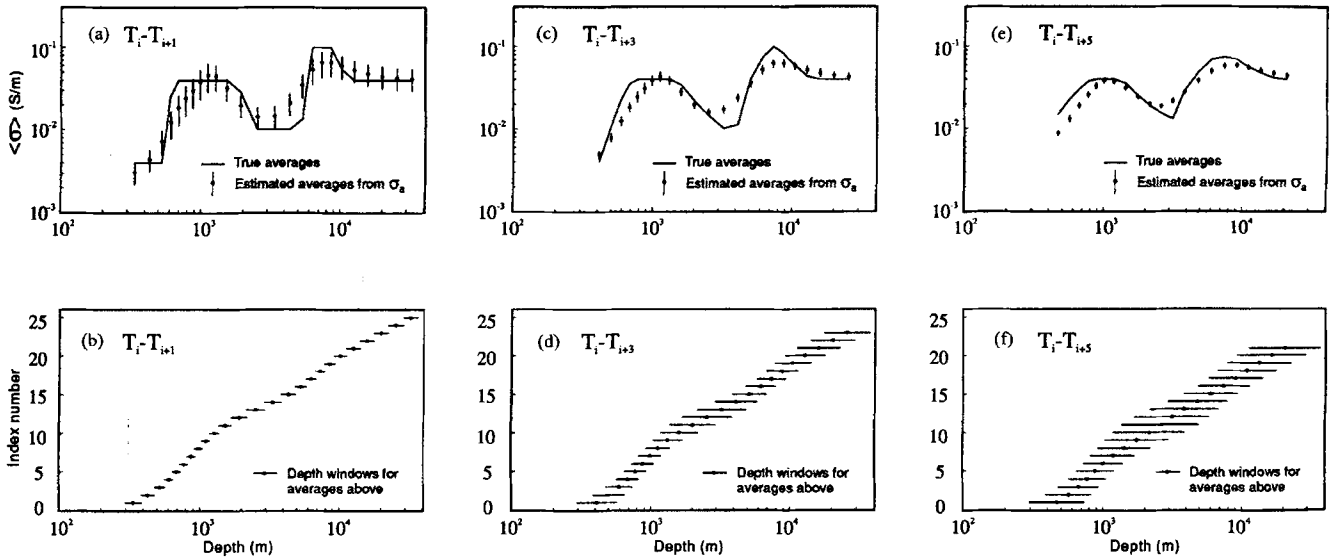


**Figure 3.** Depth averages of electrical conductivity derived from the apparent conductivity curve shown in Fig. 2. The estimated averages were computed using eq. (12). The true averages were obtained by running the corresponding windows through the original model of Fig. 2. Note that the approximation improves for the averages derived from the wider windows. Note also that in all cases the approximate averages are able to recover the five layers of the original model.

### 3 CONDUCTIVITY AVERAGES

The inference problem can be stated as the search for the common properties shared by all models fitting the observations. This means that in our case we should look for the common properties of all solutions of eq. (2) for a given set of data. The Niblett–Bostick transformation represented by eq. (5) gives one of these solutions, and other solutions can be obtained by applying different numerical methods to eq. (2). The inference problem would then consist of finding and computing the common properties of all these solutions. However, since we can never compute all possible solutions, it is clear that any valid approach must begin by defining the inference problem in its own terms. This implies that we must first select a relevant property of the models, and then find a way to compute it without going to the trouble of inspecting all possibilities. In the present work we consider the depth average of electrical conductivity between two given depths as the relevant property. This follows the general approach suggested by Parker (1983) for the exact problem. On the other hand, the computation of the averages is based on eq. (2) as originally derived by Niblett & Sayn-Wittgenstein (1960). This section shows how formulas for the average  $\bar{\sigma}(z_1, z_2)$ , for  $z_1$  and  $z_2$ , and for the variance of  $\bar{\sigma}(z_1, z_2)$  are easily constructed. All the relevant parameters of the inference problem can be evaluated directly from the data, without any assumption about the conductivity profile of the Earth.

Let us consider the problem of computing spatial averages of  $\sigma(z)$  from a given set of observations  $\sigma_a(T_i)$ ,  $i = 1, n$ . The quantity of interest is

$$\bar{\sigma}(z_1, z_2) = \frac{1}{z_2 - z_1} \int_{z_1}^{z_2} \sigma(z) dz. \quad (11)$$

Using eq. (2) for  $\sigma_a(T_1)$  and  $\sigma_a(T_2)$ , with  $T_2 > T_1$ , it is a simple matter to show that  $\bar{\sigma}(z_1, z_2)$  can be computed directly from

the data as

$$\bar{\sigma}(z_1, z_2) = [\sigma_a(T_2)\sigma_a(T_1)]^{1/2} \frac{1 - XY}{Y - X}, \quad (12)$$

where  $X = (T_1/T_2)^{1/2}$  and  $Y = [\sigma_a(T_1)/\sigma_a(T_2)]^{1/2}$ . The depths  $z_1$  and  $z_2$  are given as

$$z_1 = \left( \frac{T_1}{2\pi\mu_0\sigma_a(T_1)} \right)^{1/2} \quad (13)$$

and

$$z_2 = \left( \frac{T_2}{2\pi\mu_0\sigma_a(T_2)} \right)^{1/2}. \quad (14)$$

It is important to emphasize that the object of computing  $\bar{\sigma}(z_1, z_2)$  is not to obtain a solution of eq. (2). This goal is accomplished by using the Niblett–Bostick transformation. Rather, the object is to compute a property that is common to all possible solutions of eq. (2). This property is  $\bar{\sigma}(z_1, z_2)$ . Notice that the formula for the averages represents a non-linear combination of the data. This is a most important feature of eq. (12), whose origin can be traced back to the integral eqs (2) and (7).

It is clear that  $\bar{\sigma}(z_1, z_2)$  will have uncertainties depending on the uncertainties on  $\sigma_a$ . The situation can be controlled simply by computing the largest and the smallest values of  $\bar{\sigma}(z_1, z_2)$  that are allowed by the observations. This can be accomplished by using the extreme values of  $\sigma_a(T_1)$  and  $\sigma_a(T_2)$  in eq. (12), and then choosing the corresponding extreme values of  $\bar{\sigma}(z_1, z_2)$ . However, since we are basing our approach on an approximate relation, the conductance equation (2), it is adequate simply to apply conventional propagation of errors to establish statistical bounds on  $\bar{\sigma}(z_1, z_2)$ . Assuming that the statistical errors of  $\sigma_a(T_1)$  and  $\sigma_a(T_2)$  are not correlated, it

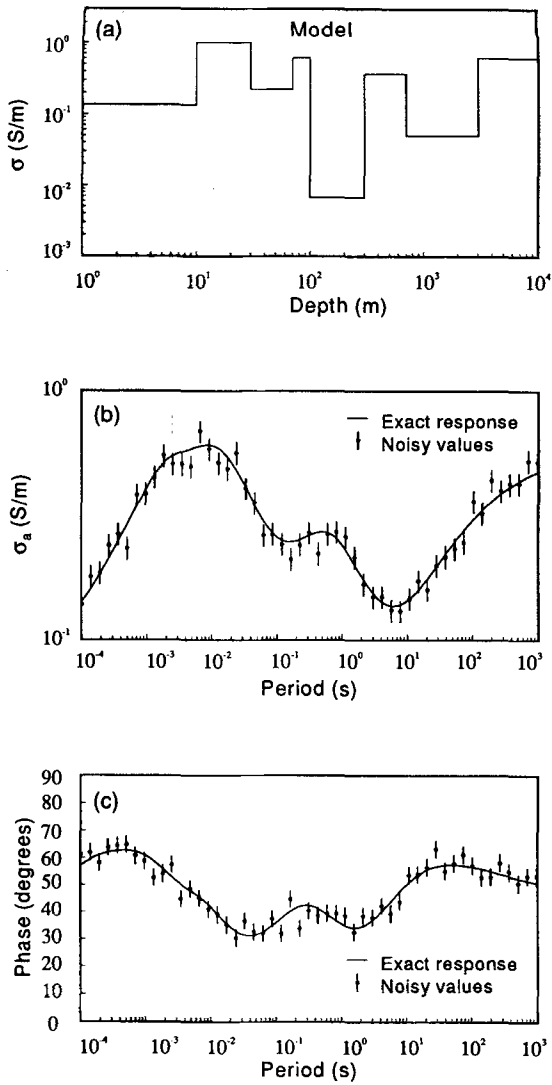


**Figure 4.** Test model and corresponding responses. The noisy values were obtained from the exact responses by adding random noise of 10 per cent to apparent conductivity and 3 degrees to phase. The scattered values are used in eqs (12) and (A9) to evaluate the performance of the formulas as stable versions of the Niblett–Bostick transformation. The results are presented in Fig. 5.

follows that

$$\begin{aligned} \text{Var}[\bar{\sigma}(z_1, z_2)] &= \left[ \frac{\partial \bar{\sigma}(z_1, z_2)}{\partial \sigma_a(T_1)} \right]^2 \text{Var}[\sigma_a(T_1)] \\ &+ \left[ \frac{\partial \bar{\sigma}(z_1, z_2)}{\partial \sigma_a(T_2)} \right]^2 \text{Var}[\sigma_a(T_2)]. \end{aligned} \quad (15)$$

The partial derivatives of  $\bar{\sigma}(z_1, z_2)$  can be easily evaluated from eq. (12). After some algebra the derivatives are

$$\frac{\partial \bar{\sigma}(z_1, z_2)}{\partial \sigma_a(T_1)} = \frac{1}{2} Y^{-2} \left\{ \frac{2X^2 - XY^{-1} - XY}{(1 - XY^{-1})^2} \right\} \quad (16)$$

and

$$\frac{\partial \bar{\sigma}(z_1, z_2)}{\partial \sigma_a(T_2)} = \frac{1}{2} \left\{ \frac{2 - XY^{-1} - XY}{(1 - XY^{-1})^2} \right\}. \quad (17)$$

With this, we can compute the upper and lower bounds of  $\bar{\sigma}(z_1, z_2)$  directly from the data.

Within the limitations imposed by the fact that the conduction equation is only an approximation, eqs (12) and (15) represent a formal solution of the general 1-D MT inference problem. In the Appendix, the solution is modified to include phase measurements. The version that uses the phase is not as general as eq. (12) because it requires interpolation between individual data points. However, it should prove useful in cases when the sounding curve is very well sampled. Before considering the performance of eqs (12) and (15), it is interesting to examine the case of a homogeneous earth to see the insight provided by the method of averages.

#### 4 HOMOGENEOUS EARTH

The expressions for  $\bar{\sigma}(z_1, z_2)$  and its variance reduce significantly for the case of a homogeneous earth. It is possible to obtain general properties of the averages by inspecting this model in detail. All measurements  $\sigma_a(T_i)$  are equal for all  $T_i$  and their value is the conductivity of the homogeneous half-space. The variance of  $\sigma_a(T_i)$  is also assumed to be the same for all periods. Eq. (12), the formula for the averages, reduces to

$$\bar{\sigma}(z_1, z_2) = \sigma_0 \quad (18)$$

for all  $z_1$  and  $z_2$ . This means that regardless of our choice of  $T_1$  and  $T_2$  we always obtain the same average value  $\sigma_0$ , as expected. The formula for the variance of  $\bar{\sigma}$  reduces to

$$\frac{\text{Var}[\bar{\sigma}(z_1, z_2)]}{\text{Var}[\sigma_a(T_i)]} = \frac{1 + (T_1/T_2)}{(1 - \sqrt{(T_1/T_2)})^2}. \quad (19)$$

The variance of  $\bar{\sigma}$  depends on our choice of  $T_1$  and  $T_2$ . As  $T_2 \rightarrow T_1$ , the variance of  $\bar{\sigma}$  increases without bound. Also, as  $T_2 \rightarrow T_1$ ,  $z_2 \rightarrow z_1$  and therefore  $\bar{\sigma}(z_1, z_2) \rightarrow \sigma(z)$ . This means that with noisy data any estimate of  $\sigma(z)$  is extremely inaccurate. In general, eq. (19) implies that as one tries to improve the space resolution of an average, one simultaneously loses precision in the determination of its value. The better the resolution, the worse the variance, and vice versa.

The resolving power of the averages can be characterized by

$$s = \frac{z_2 - z_1}{\sqrt{z_2 z_1}} = \frac{1 - (T_1/T_2)^{1/2}}{(T_1/T_2)^{1/4}}. \quad (20)$$

As  $T_2 \rightarrow T_1$ ,  $s \rightarrow 0$ , in which case we have perfect resolution. The farther apart  $T_1$  and  $T_2$  are, the larger  $s$ . It is possible to eliminate  $T_1$  and  $T_2$  from eqs (19) and (20) and to express the variance of  $\bar{\sigma}(z_1, z_2)$  directly in terms of  $s$ . The resulting equation and its graphical representation are shown in Fig. 1.

It is observed that the normalized standard deviation of  $\bar{\sigma}$  always remains above unity, regardless of the value of  $s$ . In practice, this means that we can never obtain averages with smaller errors than those of the data themselves. For  $s = 0$  the error in  $\bar{\sigma}$  is unbounded. However, because of the almost vertical behaviour of the curve, the error decreases sharply compared to the loss in resolution. Notice that the standard deviation of  $\bar{\sigma}$  decreases to less than double the standard deviation of the data at  $s = 1$ . Notice also that for  $s = 1$ ,  $T_2$  can be seven times  $T_1$ , which means that we can take two points almost one decade apart in period and still obtain averages with reasonable resolution.

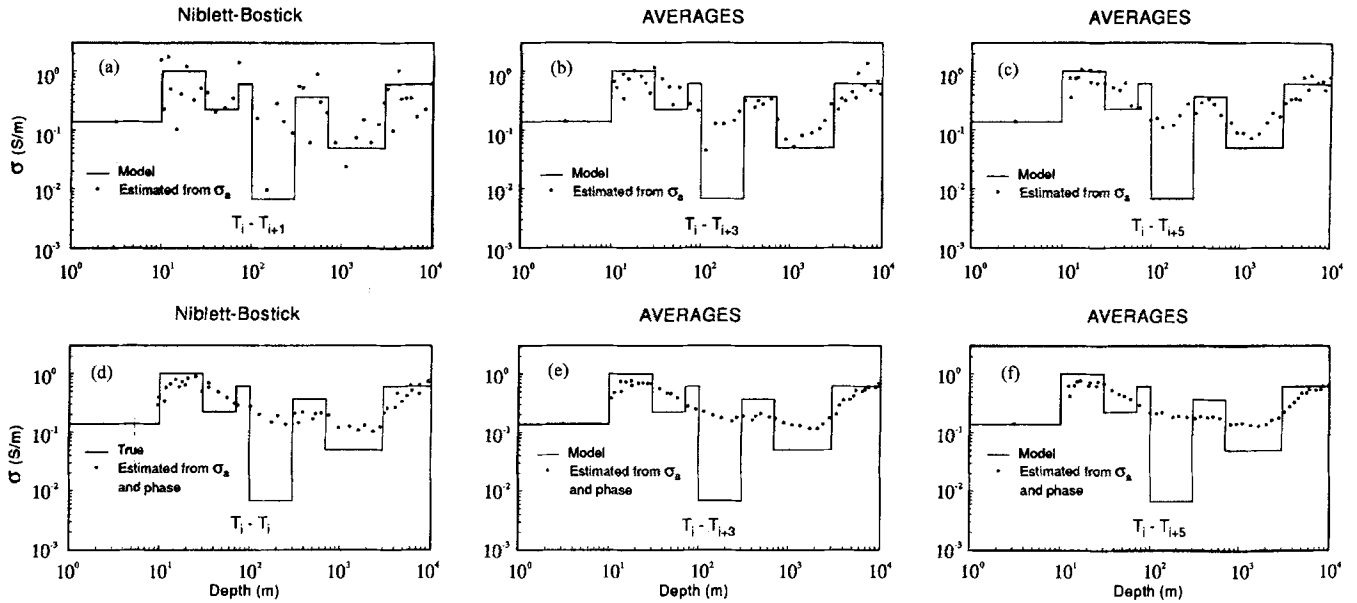


**Figure 5.** (a) and (d) show the results of applying the Niblett–Bostick transformation to the sounding curves of Fig. 4. The first case corresponds to eq. (5), which uses slope estimates, and the second to eq. (A19), which uses phase values. (b) and (c) illustrate the performance of eq. (12) for two different steps in period. (e) and (f) show the results of applying eq. (A9). The best results are obtained with eq. (12) for the step indicated in (c).

## 5 THE NIBLETT–BOSTICK TRANSFORMATION

The definition of  $\bar{\sigma}(z_1, z_2)$  given by eq. (11) and the formula to compute it from the data, eq. (12), are general expressions in the sense that they are valid for arbitrary depths  $z_1$  and  $z_2$ . In the limit as  $z_2 \rightarrow z_1$  the formula for  $\bar{\sigma}(z_1, z_2)$  should reduce to the Niblett–Bostick transformation given by eq. (5).

Let us write  $z_1 = h$  and  $z_2 = h + \Delta h$ . It is clear from eq. (11) that

$$\lim_{\Delta h \rightarrow 0} \bar{\sigma}(h, h + \Delta h) = \lim_{\Delta h \rightarrow 0} \frac{1}{\Delta h} \int_h^{h+\Delta h} \sigma(z) dz = \sigma(h). \quad (21)$$

This simply means that  $\bar{\sigma}(h) = \sigma(h)$ . Let us now consider eq. (12) for  $\bar{\sigma}(h, h + \Delta h)$  expressed in terms of the data. In this case consider that a small  $\Delta T$  corresponds to a small  $\Delta h$  because  $T$  and  $h$  are related by eq. (3). Writing  $T_1 = T$  and  $T_2 = T + \Delta T$  it follows that

$$X = \left( \frac{T}{T + \Delta T} \right)^{1/2} \approx 1 - \frac{1}{2} \frac{\Delta T}{T} \quad (22)$$

and

$$Y = \left( \frac{\sigma_a(T)}{\sigma_a(T) + \Delta \sigma_a(T)} \right)^{1/2} \approx 1 - \frac{1}{2} \frac{\Delta \sigma_a(T)}{\sigma_a(T)}. \quad (23)$$

For small increments  $\Delta T$  it also follows that

$$\sigma_a(T + \Delta T) \approx \sigma_a(T) + \frac{\partial \sigma_a(T)}{\partial T} \Delta T \quad (24)$$

or

$$\Delta \sigma_a(T) \approx \frac{\partial \sigma_a(T)}{\partial T} \Delta T. \quad (25)$$

After substitution in eq. (12) the result is

$$\bar{\sigma}(h, h + \Delta h)$$

$$= [\sigma_a(T + \Delta T) \sigma_a(T)]^{1/2} \times \frac{(\Delta T/T) + (\Delta T/\sigma_a)(\partial \sigma_a(T)/\partial T) - (\Delta T^2/2\sigma_a T)(\partial \sigma_a(T)/\partial T)}{(\Delta T/T) - (\Delta T/\sigma_a)(\partial \sigma_a(T)/\partial T)}. \quad (26)$$

Rearranging terms and taking the limit in eq. (26) according to eq. (21), the result is

$$\sigma(h) = \sigma_a(T) \frac{1 + (T/\sigma_a T)(\partial \sigma_a(T)/\partial T)}{1 - (T/\sigma_a T)(\partial \sigma_a(T)/\partial T)}, \quad (27)$$

which is equivalent to the Niblett–Bostick transformation given by eq. (5).

In the previous section we considered the special case of a homogeneous earth and showed that the variance of  $\bar{\sigma}(z_1, z_2)$  increases without bound as  $z_2 \rightarrow z_1$ . The same is true in general because expressions (16) and (17), or equivalently eq. (15), indicate that as  $T_2 \rightarrow T_1$ , the variance of  $\bar{\sigma}(z_2, z_1)$  increases without bound. We conclude that the Niblett–Bostick transformation corresponds to spatial averages with the best resolution and worst variance. This explains why the transformation tends to be unstable for noisy data. The version of eq. (27) that uses phase measurements is derived in the Appendix from the corresponding formula for the averages.

## 6 APPLICATIONS

This section describes three applications of the formulas derived above. The first is designed to address the accuracy of eq. (12) by comparing exact averages of a hypothetical model with estimations derived from the corresponding surface response. The model and the apparent conductivity and phase curves are shown in Fig. 2. The values of the responses are noise-free but they were assigned 5 per cent error bars for computing statistics. In this we follow Whittall & Oldenburg (1992), who used the same data for testing a variety of inversion

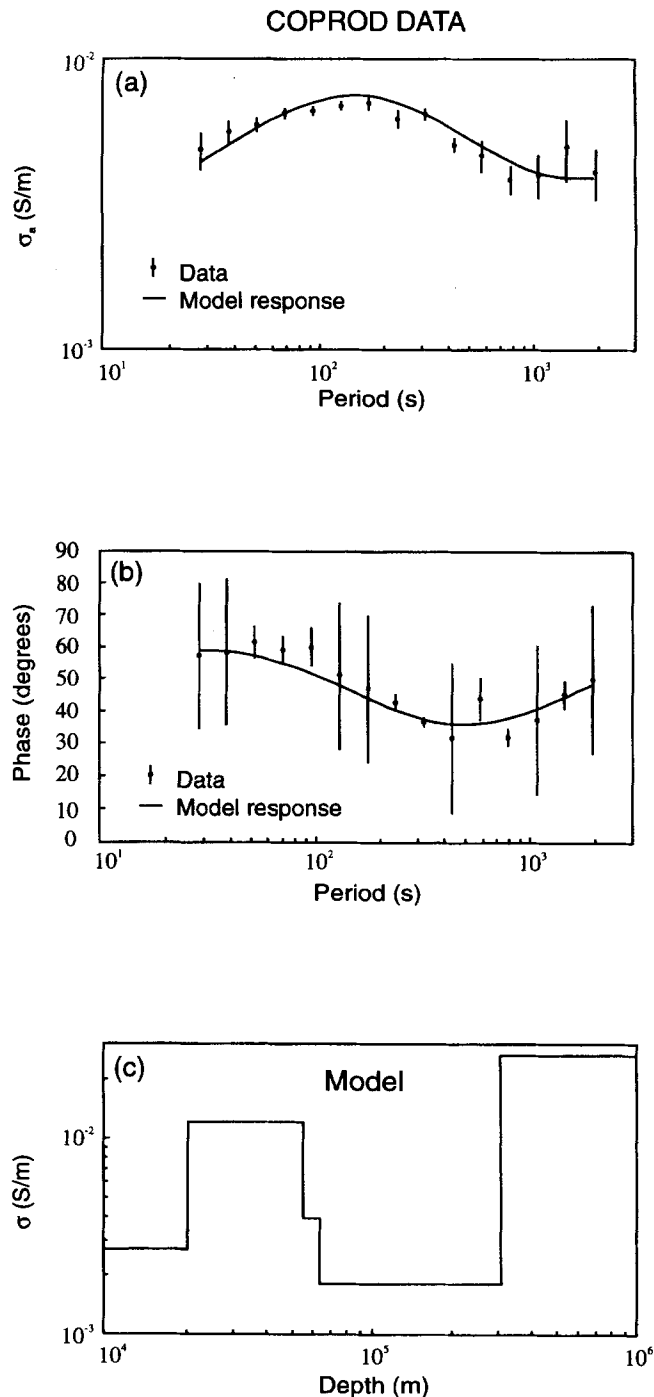


**Figure 6.** The COPROD data set after Jones & Hutton (1979). The model in (c) was obtained by inverting the data with an iterative method described in Esparza & Gómez-Treviño (1996). The depth averages derived from these data are shown in Fig. 7.

methods. They present different 1-D models that fit the data set of Fig. 2. Although the present computation of averages is not intended to produce models whose responses fit the data, it may be interesting to contrast the results with models offered by existing construction methods. We use here the same data as Whittall & Oldenburg (1992) to make the comparison easy to the reader. The first test of the present method is shown in Fig. 4. The computations are made for three different sets of

depth windows that correspond to different choices of steps in period. Given any two periods  $T_1$  and  $T_2$  ( $T_2 > T_1$ ), and two apparent conductivity values  $\sigma_a(T_1)$  and  $\sigma_a(T_2)$ , the estimated averages  $\bar{\sigma}(z_1, z_2)$  were computed using eq. (12). The depths  $z_1$  and  $z_2$  were obtained from eqs (13) and (14) respectively. The averages are plotted at the mean depth  $z = (z_1 z_2)^{1/2}$ . Fig. 3(a) was obtained using contiguous data points. This corresponds to the best possible resolution as indicated by the narrow depth windows of Fig. 3(b). Figs 3(c) to 3(f) were obtained by considering larger steps, as indicated in each case. The true averages are obtained by running the corresponding depth windows through the hypothetical model of Fig. 2(a). It is observed that the approximate values follow the true averages reasonably well in the three cases. All of the five layers of the original model are clearly preserved in the variations of the true averages, and all five layers are also recovered by the approximation. Notice how the variance of the averages decreases as the width of the windows increases. Consider now the results included in the Appendix that were obtained from amplitude and phase data. It can be observed in Fig. A1 that the estimated averages are not as good as those shown in Fig. 3. One must conclude that the averages computed from apparent conductivity data alone are more accurate than those that include phase. It is also worth noting that in all cases the width of the depth windows decreases around layers of high conductivity, and vice versa. This simply means that good conductors are better resolved than resistive layers.

The second example illustrates that the formula for the averages represents a stable alternative to the Niblett–Bostick transformation in the case of noisy data. The model and the apparent conductivity and phase curves are shown in Fig. 4. The scattered values were obtained from the exact response of the model by adding 10 per cent and 3 degrees random noise to the apparent conductivity and phase curves respectively. In this case the test model was taken from Oldenburg (1979), who used linearization and Backus–Gilbert theory for estimating spatial averages of the conductivity distribution. The model is very complicated and the diffusive nature of MT could not hope to resolve all the details, regardless of the inverse method. The reader is referred to the paper by Oldenburg (1979) for a comparison of the present results with linearized Backus–Gilbert theory. The results of the present method are shown in Fig. 5. Those corresponding to the Niblett–Bostick transformation are shown in Figs 5(a) and (d). It is observed that the formula that uses amplitude and phase data (eq. A19) is more stable than eq. (5), which requires values of the slope of the sounding curve. In Fig. 5(a) the slope was estimated using contiguous data points, which explains the widely scattered values. The smoothing effect of the phase as an independent estimate of the slope is a well-known feature of the transformation. Consider now the average values obtained from apparent conductivity data alone using eq. (12). These are shown in Figs 5(b) and (c). It is observed that the best estimates are those shown in Fig. 5(c), which corresponds to averages computed from widely spaced data. There is a lot less scattering than in Fig. 5(a) and the estimated conductivity profile is of better quality than that of Fig. 5(d). This means that using widely spaced apparent conductivity data in eq. (12) surpasses the use of phase data in the Niblett–Bostick transformation.

The third example corresponds to the application of the formulas to the well-known COPROD data set described by

## COPROD AVERAGES

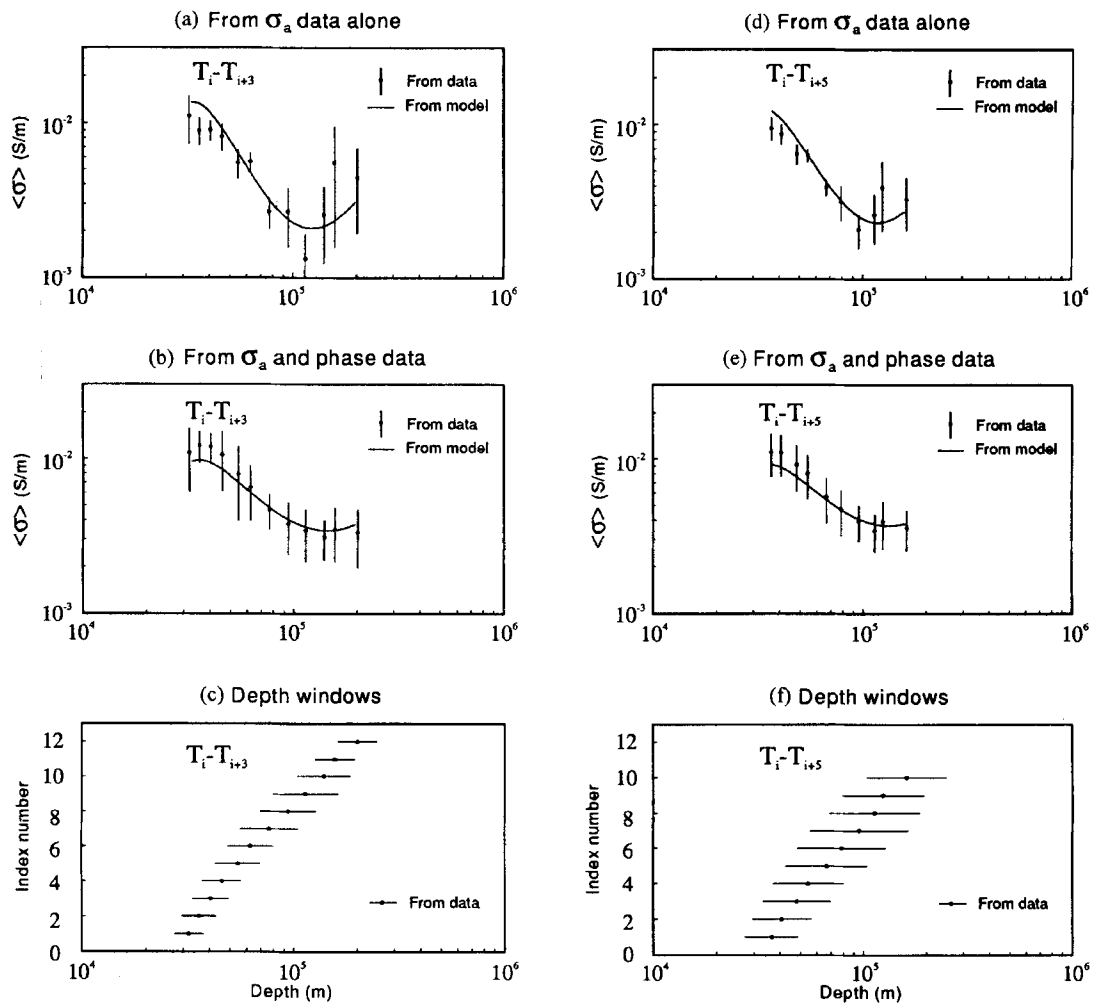


**Figure 7.** Depth averages for the COPROD data set. The continuous lines represent the average profiles derived from the response of the model shown in Fig. 6(c). It is clear, particularly in (a) and (d), that there is a trend of the scattered values to increase with depth. However, the uncertainties are too large to fully support the existence of the deep conductive layer of the model.

Jones and Hutton (1979). The apparent conductivity and phase curves are shown in Fig. 6. The model presented in Fig. 6(c) was obtained using an iterative technique described by Esparza & Gómez-Treviño (1996). The method uses linear programming to obtain a conductivity distribution whose response satisfies the exact conductance equation (7) to a required level for a given data set. There is nothing special about this model. It shows an increase in conductivity around 300 m similar to that in alternative models derived by other workers (e.g. Jones & Hutton 1979; Constable *et al.* 1987). In this application the idea is to compute averages at depth directly from the data and to see whether the results support this increase in conductivity around 300 km. The results are shown in Fig. 7. The averages computed from the data are compared with the averages computed from the response of the model of Fig. 6(c). The values computed from the response of the model (continuous line) are not strictly necessary for the analysis of the averages computed from the data. They are included here simply as a reference for the real averages. In this sense the continuous line represents the results that one

would obtain with perfect data, provided the model of Fig. 6(c) resembles the real Earth. It is observed in Fig. 7 that the continuous line shows very clearly the effect of the deep increase in conductivity. This is particularly true of the averages derived from the amplitude response. On the other hand, it is observed that the values computed from the data follow the continuous line, but it is also evident that the error bars are far too large. The conductivity averages clearly tend to increase with depth, but the size of the uncertainties do not fully support this increase. This means that from the point of view of the present analysis, the COPROD data set does not necessarily imply an increase in conductivity around 300 km. This example illustrates the type of practical issues that can be formally approached with a solution of the inference problem.

## 7 CONCLUSIONS

This paper addresses by means of a simple non-linear approximation the often neglected 1-D MT inference problem. It is



possible using equation (12) to transform a surface MT response into a depth profile of spatial conductivity averages. Each average is computed simply by combining any two data points of the sounding curve. The same data points also determine the variance and the depth range of the averages. All these parameters that define the 1-D MT inference problem can be evaluated directly from the data without any external assumption about the conductivity profile of the Earth. The main features of the method are its simplicity and its flexibility in obtaining averages with different variances and vertical profiles with varying degrees of smoothing. These vertical profiles represent spatial averages of all possible models whose responses fit the data. Any of these models can be tested to determine whether or not a particular feature is required by the data. The third example, summarized in Fig. 7, illustrates this practical application of the method using the COPROD data set.

A drawback of the method is that it is based on an approximate conductance equation. However, its main asset is that this equation retains some of the non-linear character of the problem. It is this non-linear feature that makes the formula a reasonably accurate approximation for the true averages. The first example, summarized in Fig. 3, illustrates this point by comparing the true and the approximate averages. Perhaps the method could be improved by using the exact conductance equation. However, as it stands, the approximate formula should prove useful for making inferences about the deep conductivity profile of the Earth, using no information or assumption other than the surface MT data. This independence from external assumptions distinguishes the method from existing approaches based on Backus–Gilbert theory, which require reference models when applied to the MT problem.

The formula for the averages reduces to the well-known Niblett–Bostick transformation for the case of optimal resolution and worse variance. This explains why the transformation is unstable for noisy data, and why the version that uses phase is more appropriate in such cases. In this respect, it is shown that using widely spaced apparent conductivity data in the formula for the averages surpasses the use of phase in the transformation. The second example, summarized in Fig. 5, illustrates this point. On the other hand, considering the relative success of the approximation, it would be interesting to consider its possible extension to the multidimensional cases. Along this line, so far we know that an imaging technique based on a generalized two-dimensional version of the Niblett–Bostick transformation produces reasonably good models from a given data set (Esparza *et al.* 1993). The problem still remains of devising effective algorithms for computing the averages and their variances. However, apart from any possible generalizations to the multidimensional cases, it is to be hoped that the present treatment of the 1-D MT inference problem could widen the interest for its solution within the electromagnetic community.

#### ACKNOWLEDGMENTS

I am grateful to F. Esparza and M. Mondragón for fruitful discussions, and to S. Méndez for critically reading the final version of the manuscript.

#### REFERENCES

- Backus, G.E. & Gilbert, J.F., 1970. Uniqueness in the inversion of inaccurate gross earth data, *Phil. Trans. R. Soc. Lond., A*, **266**, 123–150.
- Bahr, K., Olsen, N. & Shankland, T.J., 1993. On the combination of magnetotelluric and geomagnetic depth sounding method for resolving an electrical conductivity increase at 400 km depth, *Geophys. Res. Lett.*, **20**, 2937–2940.
- Bostick, F.X., 1977. A simple almost exact method of magnetotelluric analysis, in *Workshop on Electrical Methods in Geothermal Exploration*, US Geol. Surv., Contract No. 14080001-G-359.
- Constable, S.C., Parker, R.L. & Constable, C.G., 1987. Occam's inversion: A practical algorithm for generating smooth models from electromagnetic sounding data, *Geophysics*, **52**, 289–300.
- Dmitriev, V.I., 1983. Inverse problems in electrodynamic prospecting, in *Ill-Posed Problems in the Natural Sciences*, pp. 77–101, eds Tikhonov, A.N. & Goncharsky, A.V., Mir Publishers, Moscow.
- Esparza, F.J. & Gómez-Treviño, E., 1996. Inversion of magnetotelluric soundings using a new integral form of the induction equation, *Geophys. J. Int.*, **127**, 452–460.
- Esparza, F.J., Pérez-Flores, M.A., Gallardo, L.A. & Gómez-Treviño, E., 1993. A simple method of magnetotelluric inversion in two dimensions, *Expanded Abstracts, 3rd Int. Congress Brazilian Geophys. Soc.*, **2**, 1461–1463.
- Goldberg, S. & Rotstein, Y., 1982. A simple form of presentation of magnetotelluric data using the Bostick transform, *Geophys. Prospect.*, **30**, 211–216.
- Gómez-Treviño, E., 1987. Nonlinear integral equations for electromagnetic inverse problems, *Geophysics*, **52**, 1297–1302.
- Gómez-Treviño, E., 1992. A simple method of magnetotelluric inversion: Average models, conductivity bounds and resolution directly from the data, presented at the *11th IAGA Workshop on Electromagnetic Induction in the Earth*, Wellington, New Zealand.
- Jones, A.G., 1983. On the equivalence of the Niblett and Bostick transformation in the magnetotelluric method, *Z. Geophys.*, **53**, 72–73.
- Jones, A.G. & Hutton, R., 1979. A multi-station magnetotelluric study in southern Scotland—II. Monte-Carlo inversion of the data and its geophysical and tectonic implications, *Geophys. J. R. astr. Soc.*, **56**, 351–368.
- Niblett, E.R. & Sayn-Wittgenstein, C., 1960. Variation of electrical conductivity with depth by the magnetotelluric method, *Geophysics*, **25**, 998–1008.
- Oldenburg, D.W., 1979. One-dimensional inversion of natural source magnetotelluric observations, *Geophysics*, **44**, 1218–1244.
- Oldenburg, D.W., 1983. Funnel functions in linear and nonlinear appraisal, *J. geophys. Res.*, **88**, 7387–7398.
- Parker, R.L., 1970. The inverse problem of electrical conductivity in the mantle, *Geophys. J. R. astr. Soc.*, **22**, 121–138.
- Parker, R.L., 1983. The magnetotelluric inverse problem, *Geophys. Surv.*, **6**, 5–25.
- Schultz, A., Kurtz, R.D., Chave, A.D. & Jones, A.G., 1993. Conductivity discontinuities in the upper mantle beneath a stable craton, *Geophys. Res. Lett.*, **20**, 2941–2944.
- Smith, J.T. & Booker, J.R., 1988. Magnetotelluric inversion for minimum structure, *Geophysics*, **53**, 1565–1576.
- Weaver, J.T. & Agarwal, A.K., 1993. Automatic 1-D inversion of magnetotelluric data by the method of modelling, *Geophys. J. Int.*, **112**, 115–123.
- Weidelt, P., 1972. The inverse problem of geomagnetic induction, *Z. Geophys.*, **38**, 257–289.
- Weidelt, P., 1985. Construction of conductance bounds from magnetotelluric impedances, *Z. Geophys.*, **57**, 191–206.
- Weidelt, P., 1992. Exact and approximate bounds on spatial averages of the electrical conductivity using a priori information, presented at the *11th IAGA Workshop on Electromagnetic Induction in the Earth*, Wellington, New Zealand.

Whittall, K.P. & Oldenburg, D.W., 1992. Inversion of magnetotelluric data for a one-dimensional conductivity, *Geophys. Monogr. Ser.* 5, ed. Fitterman, D.V., Soc. Exp. Geophysicists, Tulsa, OK.

## APPENDIX A: CONDUCTIVITY AVERAGES USING PHASE DATA

Eqs (12) and (15) use only amplitude measurements. All computations are performed by combining the values of any two given data points without using the information in between. The intermediate data points are not used simply because they are not required in the computation of the averages. The simplicity of the resulting formulas is of course an asset of the method. Unfortunately, when considering phase measurements the formulas become more complicated. Not only do the intermediate points enter into the picture, but they are also required in order to make an assumption about the behaviour of the phase curve between adjacent data points. That is, in order to compute the averages it is necessary to make assumptions external to the observations. The method is then less rigorous than the version that uses amplitude data alone. Nevertheless, the derivation of the formula has some interesting features regarding the variance of the averages when using measurements from a single period. The formula should also prove useful in practice as a means of comparison of eq. (12) with another approximation.

The formula for the average is given as

$$\bar{\sigma}(z_1, z_2) = [\sigma_a(T_2)\sigma_a(T_1)]^{1/2} \frac{1 - XY}{Y - X}, \quad (\text{A1})$$

where

$$X = (T_1/T_2)^{1/2} \quad (\text{A2})$$

and

$$Y = [\sigma_a(T_1)/\sigma_a(T_2)]^{1/2}. \quad (\text{A3})$$

The averages depend on the product and the ratio of  $\sigma_a(T_2)$  and  $\sigma_a(T_1)$ . The ratio of these two quantities can be expressed in terms of the phase of the impedance using an approximate relationship derived by Weidelt (1972). The original relationship derived by Weidelt (1972) can be written as

$$\frac{\partial \log \sigma_a(T)}{\partial \log T} = \frac{4}{\pi} \phi(T) - 1. \quad (\text{A4})$$

Integrating both sides with respect to  $\log T$  from  $T_1$  to  $T_2$ , the result is

$$\log \frac{\sigma_a(T_2)}{\sigma_a(T_1)} = \log \frac{T_1}{T_2} + \frac{4}{\pi} \int_{T_1}^{T_2} \phi(T) d \log T. \quad (\text{A5})$$

From this it follows that

$$Y = \left( \frac{\sigma_a(T_1)}{\sigma_a(T_2)} \right)^{1/2} = X^{-1} e^{-p}, \quad (\text{A6})$$

where

$$p = \frac{2}{\pi} \int_{T_1}^{T_2} \phi(T) d \log T. \quad (\text{A7})$$

It is clear from eq. (A7) that we require all the available phase values between  $T_1$  and  $T_2$ .

Furthermore, we need to make some assumption about the behaviour of  $\phi(T)$  between adjacent points in order to evaluate

the integral. In the present context, the reasonable thing to do is to consider the simplest assumption by evaluating the integral using rectangular boxes defined by the intervals in period and of height equal to the mean value of the two phases. That is,

$$p = \frac{2}{\pi} \sum_{i=1}^{m-1} \left( \frac{\phi(T_i) + \phi(t_{i+1})}{2} \right) \log \frac{t_{i+1}}{t_i}, \quad (\text{A8})$$

where there are  $m$  data points between  $T_1$  and  $T_2$  including the extreme points, so that  $t_1 = T_1$  and  $t_m = T_2$ . The formula for the averages then reduces to

$$\bar{\sigma}(z_1, z_2) = [\sigma_a(T_2)\sigma_a(T_1)]^{1/2} \frac{1 - e^{-p}}{X^{-1} e^{-p} - X}, \quad (\text{A9})$$

where  $p$  is as in eq. (A8). It can be easily shown that eq. (A9) reduces to the conductivity of a homogeneous half-space when the phase is uniform and equal to  $\pi/4$ , since in this case  $e^{-p} = X$ .

To obtain the formula for the variance of  $\bar{\sigma}(z_1, z_2)$ , consider that in this case  $\bar{\sigma}$  depends on both apparent conductivity and phase data. The corresponding formula can be written as

$$\begin{aligned} \text{Var}[\bar{\sigma}(z_1, z_2)] &= A^2 \text{Var}[\sigma_a(T_1)] + B^2 \text{Var}[\sigma_a(T_2)] \\ &\quad + \sum_{i=1}^m C_i^2 \text{Var}[\phi(t_i)], \end{aligned} \quad (\text{A10})$$

where

$$A = \frac{\partial \bar{\sigma}(z_1, z_2)}{\partial \sigma_a(T_1)} = \frac{1}{2} \left[ \frac{\sigma_a(T_2)}{\sigma_a(T_1)} \right]^{1/2} \frac{1 - e^{-p}}{X^{-1} e^{-p} - X}, \quad (\text{A11})$$

$$B = \frac{\partial \bar{\sigma}(z_1, z_2)}{\partial \sigma_a(T_2)} = \frac{1}{2} \left[ \frac{\sigma_a(T_1)}{\sigma_a(T_2)} \right]^{1/2} \frac{1 - e^{-p}}{X^{-1} e^{-p} - X}, \quad (\text{A12})$$

$$C_1 = D \log(t_2/t_1), \quad (\text{A13})$$

$$C_m = D \log(t_m/t_{m-1}), \quad (\text{A14})$$

and for intermediate data points

$$C_i = D \log(t_{i+1}/t_{i-1}), \quad (\text{A15})$$

where

$$D = [\sigma_a(T_2)\sigma_a(T_1)]^{1/2} \left[ \frac{1 - X^2}{(X^{-1} e^{-p} - X)^2} \right] \frac{X^{-1} e^{-p}}{\pi}. \quad (\text{A16})$$

It is of interest to consider the case of measurements at a single period. The formula for the variance of the averages can be obtained by taking the appropriate limit in eq. (A10), and then doubling the result. A factor of two is required because the formula assumes at least two independent measurements, and as  $T_2 \rightarrow T_1$  the two become one and the same. The variance is then too small by a factor of two compared to the case of a single measurement. Consider that as  $T_2 \rightarrow T_1$ ,

$$p = \frac{2}{\pi} \phi(T) \log \frac{T + \Delta T}{T} \approx \frac{2}{\pi} \phi(T) \frac{\Delta T}{T}, \quad (\text{A17})$$

where  $T_1 = T$  and  $T_2 = T + \Delta T$ . Substituting in (A10) and considering first-order expansions in  $X$ , the formula for the variance reduces to

$$\text{Var}[\sigma(h)] = \left( \frac{2\phi}{\pi - 2\phi} \right)^2 \text{Var}(\sigma_a) + \sigma_a^2 \left[ \frac{2\pi}{(\pi - 2\phi)^2} \right]^2 \text{Var}(\phi). \quad (\text{A18})$$

The most important consideration regarding the use of

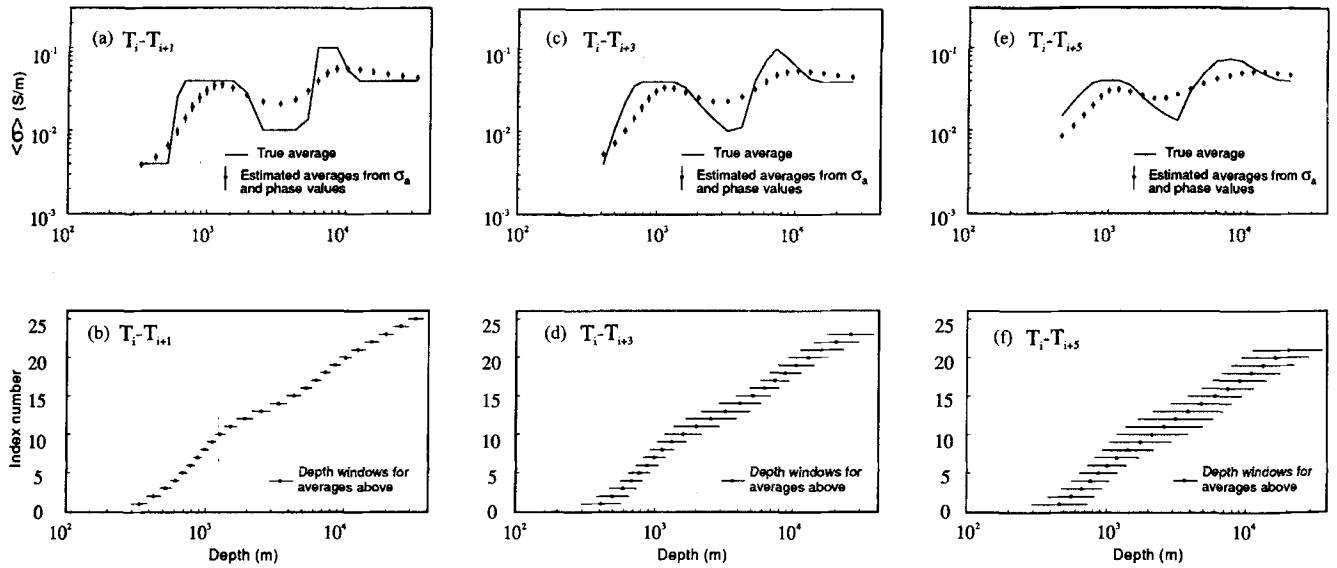


**Figure A1.** Depth averages of electrical conductivity derived from the apparent conductivity and phase curves shown in Fig. 2. The estimated averages were computed using eq. (A9). The true averages were obtained by running the corresponding windows through the original model of Fig. 2. Notice that the approximation is not as good as that shown in Fig. 3.

phase is that as  $T_2 \rightarrow T_1$ , the variances of the averages remain bounded, as opposed to the case when using only amplitude data. The reason for this difference is that phase measurements represent independent estimations of the slope of the amplitude curve at a point. This is obviously a major difference, because the slope of a curve cannot be determined accurately from two nearby inaccurate data points. However, it is important to notice that eq. (A18) is far too optimistic because it bounds the conductivity at depth. This contradicts what we know, that conductivity cannot be bounded at depth using magnetotelluric data. In this respect eqs (12) and (15) are more appropriate.

The corresponding formula for the conductivity can be obtained by substituting eq. (A17) in eq. (A9) and by taking

the appropriate limits. The result is

$$\bar{\sigma}(z_1, z_2) = \sigma(h) = \sigma_a(T) \frac{2\phi}{\pi - 2\phi}. \tag{A19}$$

As expected, the formula for the averages reduces to the Niblett–Bostick transformation as  $T_2 \rightarrow T_1$ , in the version that uses phase measurements (Bostick 1977; Goldberg & Rotstein 1982).

The results of applying eqs (A9) and (A10) to the data shown in Fig. 2 are illustrated in Fig. A1. It is observed that the profiles are too smooth and that they are not as good estimates of the true averages as those shown in Fig. 3.